

Light-Front Holography and QCD Hadronization at the Amplitude Level[★]

Stanley J. Brodsky

SLAC National Accelerator Laboratory, Stanford University, Stanford, CA 94309, USA

Guy F. de Téramond

Universidad de Costa Rica, San José, Costa Rica

Abstract

Light-front holography allows hadronic amplitudes in the AdS/QCD fifth dimension to be mapped to frame-independent light-front wavefunctions of hadrons in physical space-time, thus providing a relativistic description of hadrons at the amplitude level. The AdS coordinate z is identified with an invariant light-front coordinate ζ which separates the dynamics of quark and gluon binding from the kinematics of constituent spin and internal orbital angular momentum. The result is a single-variable light-front Schrödinger equation for QCD which determines the eigenspectrum and the light-front wavefunctions of hadrons for general spin and orbital angular momentum. A new method for computing the hadronization of quark and gluon jets at the amplitude level using AdS/QCD light-front wavefunctions is outlined.

Key words: AdS/CFT, QCD, Holography, Light-Front Wavefunctions, Hadronization

PACS: 11.15.Tk, 11.25Tq, 12.38Aw, 12.40Yx

1. Introduction

The AdS/CFT correspondence [1] between string states in anti-de Sitter (AdS) space and conformal field theories in physical space-time, modified for color confinement, has led to semiclassical models for strongly-coupled QCD which provide analytical insight

[★] This research was supported by the Department of Energy contract DE-AC02-76SF00515. SLAC-PUB-13504.

Email addresses: sjbth@slac.stanford.edu (Stanley J. Brodsky), gdt@asterix.crnet.cr (Guy F. de Téramond).

into its inherently non-perturbative nature, as well as predictions for hadronic spectra, decay constants, form factors and wavefunctions.

We have recently shown [2,3] that there is a remarkable correspondence between the AdS description of hadrons and the Hamiltonian formulation of QCD in physical space-time quantized on the light front. A key feature is “light-front holography” which allows one to precisely map the AdS₅ solutions $\Phi(z)$ for hadronic amplitudes in the fifth dimensional variable z to light-front hadron wavefunctions $\psi_{n/H}(\zeta)$ in physical space-time evaluated at fixed light-front time $\tau = t + z/c$ [2,3]. For two particles $\zeta^2 = \mathbf{b}_\perp^2 x(1-x)$, which is conjugate to the invariant mass squared $\mathcal{M}^2 = \mathbf{k}_\perp^2/x(1-x)$. Light-front holography thus allows hadronic amplitudes in the AdS/QCD fifth dimension to be mapped to amplitudes in physical space-time. One can derive this connection by showing that one obtains the identical holographic mapping for matrix elements of the electromagnetic current and the energy-momentum tensor [4]. The mathematical consistency of light-front holography for both the electromagnetic and gravitational [4] hadronic transition matrix elements demonstrates that the mapping between the AdS holographic variable z and the light-front variable ζ , is a general principle.

Some of the important features of light-front AdS/QCD include: (a) Effective frame-independent single-particle Schrödinger and Dirac equations for meson and baryon wave equations in both z and ζ . For example, the meson eigenvalue equation is

$$\left[-\frac{d^2}{dz^2} - \frac{1-4L^2}{4z^2} + U(z) \right] \phi(z) = \mathcal{M}^2 \phi(z), \quad (1)$$

where the soft-wall potential has the form of a harmonic oscillator $U(z) = \kappa^4 z^2 + 2\kappa^2(L+S-1)$. (b) The mass spectra formula for mesons at zero quark mass in the soft-wall model is $\mathcal{M}^2 = 4\kappa^2(n+L+S/2)$, which agrees with conventional Regge phenomenology. As in the Nambu string model based on a rotating flux tube, the Regge slope is the same for both the principal quantum number n and the orbital angular momentum L . The AdS/QCD correspondence thus builds in a remarkable connection between the string mass μ in the string theory underlying an effective gravity theory in the fifth dimension with the orbital angular momentum of hadrons in physical space-time. (c) The pion is massless at zero quark mass in agreement with general arguments based on chiral symmetry. (d) The predicted form factors for the pion and nucleons agree well with experiment. The nucleon LFWFs have both S - and P - wave components, allowing one to compute both Dirac and Pauli form factors. In general the AdS/QCD form factors fall off in momentum transfer squared q^2 with a leading power predicted by dimensional counting rules and the leading twist of the hadron’s dominant interpolating operator at short distances. Under conformal transformations the interpolating operators transform according to their twist, and consequently the AdS isometries map the twist scaling dimensions into the AdS modes [5]. Light-front holography thus provides a simple semiclassical approximation to QCD which has both constituent counting rule behavior [6,7] at short distances and confinement at large distances [8,9]. (e) The timelike form factors of hadrons exhibit poles in the $J^{PC} = 1^{--}$ vector meson channels, an analytic feature which arises from the dressed electromagnetic current in AdS/QCD [3,10]. (f) The form of the nonperturbative pion distribution amplitude $\phi_\pi(x)$ obtained from integrating the $q\bar{q}$ valence LFWF $\psi(x, \mathbf{k}_\perp)$ over \mathbf{k}_\perp , has a quite different x -behavior than the asymptotic distribution amplitude predicted from the ERBL PQCD evolution [11,12] of the pion distribution amplitude. The AdS prediction $\phi_\pi(x) = \sqrt{3}f_\pi \sqrt{x(1-x)}$ has a broader

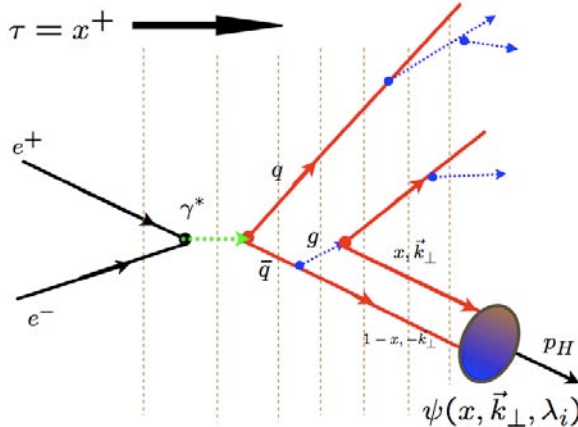


Fig. 1. Illustration of an event amplitude generator for $e^+e^- \rightarrow \gamma^* \rightarrow X$ for hadronization processes at the amplitude level. Capture occurs if $\zeta^2 = x(1-x)\mathbf{k}_\perp^2 > 1/\Lambda_{\text{QCD}}^2$ in the AdS/QCD hard-wall model of confinement; i.e., if $\mathcal{M}^2 = \mathbf{k}_\perp^2/x(1-x) < \Lambda_{\text{QCD}}^2$.

distribution than expected from solving the ERBL evolution equation in perturbative QCD. This observation appears to be consistent with the results of the Fermilab diffractive dijet experiment [13], the moments obtained from lattice QCD [8], and pion form factor data [14].

2. Hadronization at the Amplitude Level

The conversion of quark and gluon partons is usually discussed in terms of on-shell hard-scattering cross sections convoluted with *ad hoc* probability distributions. The LF Hamiltonian formulation of quantum field theory provides a natural formalism to compute hadronization at the amplitude level [15]. In this case one uses light-front time-ordered perturbation theory for the QCD light-front Hamiltonian to generate the off-shell quark and gluon T-matrix helicity amplitude using the LF generalization of the Lippmann-Schwinger formalism:

$$T^{LF} = H_I^{LF} + H_I^{LF} \frac{1}{\mathcal{M}_{\text{initial}}^2 - \mathcal{M}_{\text{intermediate}}^2 + i\epsilon} H_I^{LF} + \dots \quad (2)$$

Here $\mathcal{M}_{\text{intermediate}}^2 = \sum_{i=1}^N (\mathbf{k}_{\perp i}^2 + m_i^2)/x_i$ is the invariant mass squared of the intermediate state and H_I^{LF} is the set of interactions of the QCD LF Hamiltonian in the ghost-free light-cone gauge [16]. The T^{LF} matrix elements are evaluated between the out and in eigenstates of H_{LF}^{QCD} . The LFWFs of AdS/QCD can be used as the interpolating amplitudes between the off-shell quark and gluons and the bound-state hadrons. Specifically, if at any stage a set of color-singlet partons has light-front kinetic energy $\sum_i \mathbf{k}_{\perp i}^2/x_i < \Lambda_{\text{QCD}}^2$, then one coalesces the virtual partons into a hadron state using the AdS/QCD LFWFs. This provides a specific scheme for determining the factorization scale which matches perturbative and nonperturbative physics. The event amplitude generator is illustrated for $e^+e^- \rightarrow \gamma^* \rightarrow X$ in Fig. 1.

This scheme has a number of important computational advantages:

(a) Since propagation in LF Hamiltonian theory only proceeds as τ increases, all particles propagate as forward-moving partons with $k_i^+ \geq 0$. There are thus relatively few contributing τ -ordered diagrams.

(b) The computer implementation can be highly efficient: an amplitude of order g^n for a given process only needs to be computed once. In fact, each non-interacting cluster within T^{LF} has a numerator which is process independent; only the LF denominators depend on the context of the process.

(c) Each amplitude can be renormalized using the “alternate denominator” counterterm method [17], rendering all amplitudes UV finite.

(d) The renormalization scale in a given renormalization scheme can be determined for each skeleton graph even if there are multiple physical scales.

(e) The T^{LF} matrix computation allows for the effects of initial and final state interactions of the active and spectator partons. This allows for novel leading-twist phenomena such as diffractive DIS, the Siverson spin asymmetry and the breakdown of the PQCD Lam-Tung relation in Drell-Yan processes.

(f) ERBL and DGLAP evolution are naturally incorporated, including the quenching of DGLAP evolution at large x_i where the partons are far off-shell.

(g) Color confinement can be incorporated at every stage by limiting the maximum wavelength of the propagating quark and gluons.

This method retains the quantum mechanical information in hadronic production amplitudes which underlie Bose-Einstein correlations and other aspects of the spin-statistics theorem. Thus Einstein-Podolsky-Rosen quantum theory correlations are maintained, even between far-separated hadrons and clusters [18]. A similar off-shell T-matrix approach was used to predict antihydrogen formation from virtual positron-antiproton states produced in $\bar{p}A$ collisions [19].

References

- [1] J. M. Maldacena, *Adv. Theor. Math. Phys.* **2**, 231 (1998) [*Int. J. Theor. Phys.* **38**, 1113 (1999)] [arXiv:hep-th/9711200].
- [2] S. J. Brodsky and G. F. de Teramond, *Phys. Rev. Lett.* **96**, 201601 (2006) [arXiv:hep-ph/0602252].
- [3] S. J. Brodsky and G. F. de Teramond, *Phys. Rev. D* **77**, 056007 (2008) [arXiv:0707.3859 [hep-ph]].
- [4] S. J. Brodsky and G. F. de Teramond, *Phys. Rev. D* **78**, 025032 (2008) [arXiv:0804.0452 [hep-ph]].
- [5] S. J. Brodsky and G. F. de Teramond, *Phys. Lett. B* **582**, 211 (2004) [arXiv:hep-th/0310227].
- [6] S. J. Brodsky and G. R. Farrar, *Phys. Rev. Lett.* **31**, 1153 (1973).
- [7] V. A. Matveev, R. M. Muradian and A. N. Tavkhelidze, *Lett. Nuovo Cim.* **7**, 719 (1973).
- [8] S. J. Brodsky and G. F. de Teramond, arXiv:0802.0514 [hep-ph].
- [9] J. Polchinski and M. J. Strassler, *Phys. Rev. Lett.* **88**, 031601 (2002) [arXiv:hep-th/0109174].
- [10] H. R. Grigoryan and A. V. Radyushkin, *Phys. Rev. D* **76**, 095007 (2007) [arXiv:0706.1543 [hep-ph]].
- [11] G. P. Lepage and S. J. Brodsky, *Phys. Lett. B* **87**, 359 (1979).
- [12] A. V. Efremov and A. V. Radyushkin, *Phys. Lett. B* **94**, 245 (1980).
- [13] E. M. Aitala *et al.* [E791 Collaboration], *Phys. Rev. Lett.* **86**, 4768 (2001) [arXiv:hep-ex/0010043].
- [14] H. M. Choi and C. R. Ji, *Phys. Rev. D* **74**, 093010 (2006) [arXiv:hep-ph/0608148].
- [15] S. J. Brodsky, G. de Teramond and R. Shrock, *AIP Conf. Proc.* **1056**, 3 (2008) [arXiv:0807.2484 [hep-ph]].
- [16] S. J. Brodsky, H. C. Pauli and S. S. Pinsky, *Phys. Rept.* **301**, 299 (1998) [arXiv:hep-ph/9705477].
- [17] S. J. Brodsky, R. Roskies and R. Suaya, *Phys. Rev. D* **8**, 4574 (1973).
- [18] B. I. Abelev, *et al.*, arXiv:0812.1063 [nucl-ex].
- [19] C. T. Munger, S. J. Brodsky and I. Schmidt, *Phys. Rev. D* **49**, 3228 (1994).